1290
FACULDADE DE CIÊNCIAS E TECNOLOGIA
UNIVERSIDADE DE COIMBRA

PREDICTION OF FATIGUE CRACK GROWTH USING A DAMAGE MODEL

E. R. Sérgio[1] • M. F. Borges[1] • D. M. Neto[1] • F. V. Antunes[1]

[1]CEMMPRE, Department of Mechanical Engineering, University of Coimbra, Portugal

IGF26
26th International Conference on Fracture and Structural Integrity

26th-28th May 2021
Turin (Italy) & Web

Fatigue Crack Growth Mechanisms

- Typically, the fatigue crack growth rate is defined by da/dN-ΔK curves, assuming that ΔK is the crack driving force.
- These curves cannot be used to predict the effect of **stress ratio** or **variable amplitude loading**. In fact, the great success of K in last decades obscured the fundamental understanding of FCG.
- A way of understanding FCG is simulating the **crack tip phenomena**, which are effectively responsible for crack progression.

Crack Tip Plastic Deformation

- **Crack tip plastic deformation** is assumed to be the main mechanism acting at the cyclic plastic deformation, which zone may be considered the process zone.
- In the occurrence of high plastic deformations, **damage** tends to occur in the materials due to the plasticity by itself and to the processes of nucleation, growth and coalescence of micro-voids.
- This study pretends to access the influence of the **GTN damage** model on the existing FEM model, that simulates FCG through a **node release method**. Propagation occurs when the cumulative plastic strain reaches a critical value.

This study aimed the prediction of crack propagation of the 2024-T351 aluminum alloy.

All numerical simulations were performed with the in-house finite element code DD3IMP.

Material Constitutive Model

- The isotropic elastic behavior was given by the generalized **Hooke's law**. The shape of the yield surface was defined by the **von Mises** yield criterion with an associated flow rule.
- The evolution of the yield surface was described by the **Swift** isotropic hardening law combined with **Armstrong–Frederick** kinematic hardening law.

$$Y(\bar{\varepsilon}^{p}) = K\left(\left(\frac{Y_0}{K}\right)^{\frac{1}{n}} + \bar{\varepsilon}^{\mathrm{p}}\right)^{n}$$

Swift hardening law

$$\dot{\boldsymbol{X}} = C_{\mathrm{X}}\left[\frac{X_{\mathrm{sat}}}{\bar{\sigma}}(\boldsymbol{\sigma}' - \boldsymbol{X})\right]\dot{\bar{\epsilon}}_{\mathrm{pl}}$$

Armstrong–Frederick kinematic hardening law

Material Parameters

- The isotropic and kinematic hardening parameters were simultaneously calibrated using the stress–strain curves obtained in smooth specimens of the experimental low cycle fatigue tests

Elastic properties of 2024-T351 aluminium alloy and parameters for the Swift isotropic hardening law combined with the Armstrong–Frederick kinematic hardening law.

Material	E [GPa]	ν	Y_0 [MPa]	K [MPa]	n	X_{sat} [MPa]	C_X
AA 2024-T351	72.26	0.29	288.96	389.00	0.056	111.84	138.80

The twelve parameters of the GTN model for the of 2024-T351 aluminium alloy.

Material	ε_N	σ_P	s_N	s_P	f_N	f_P	q_1	q_2	q_3	f_c	f_f	f_0
AA 2024-T351	0.25	800	0.1	250	0	0	1.5	1	2.25	-	-	0.01

Geometry and Discretization

- Compact tension specimens were adopted in this study. **Plane strain** boundary conditions were applied in the numerical simulations.
- The mesh of the specimen considers three distinct zones: a very refined area near the crack tip, a transition zone, and a coarser mesh in the far side of the crack zone.
- 7287 3D solid linear isoparametric elements and 14918 nodes were used.

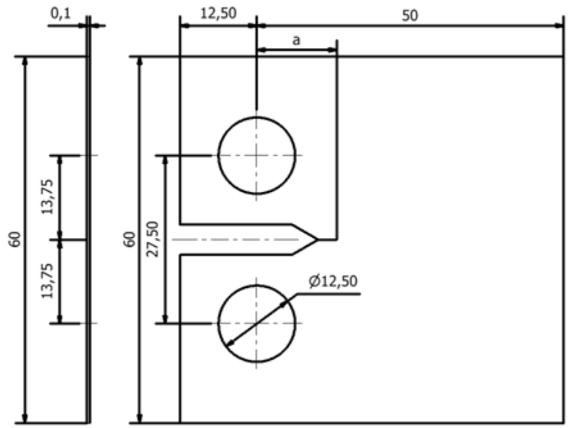

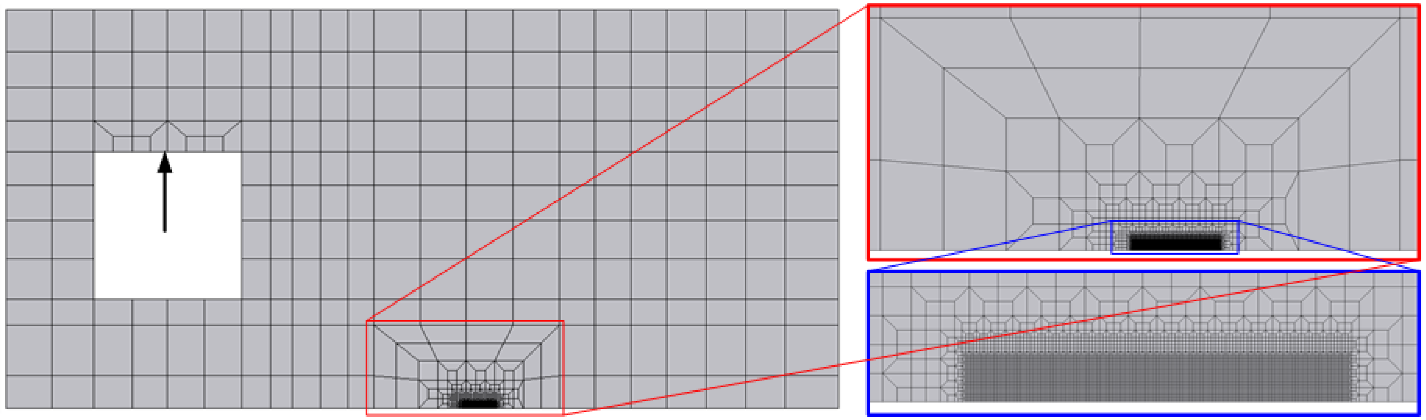

da/dN-ΔK curves

- It was expected that the introduction of the GTN damage model would result in an increase in the FCGR, particularly for high values of ΔK.
- Surprisingly, for lower values of ΔK, the GTN model has a protective behavior, reducing the FCGR.
- At some point this behavior is inverted and a faster propagation is achieved with the damage model.

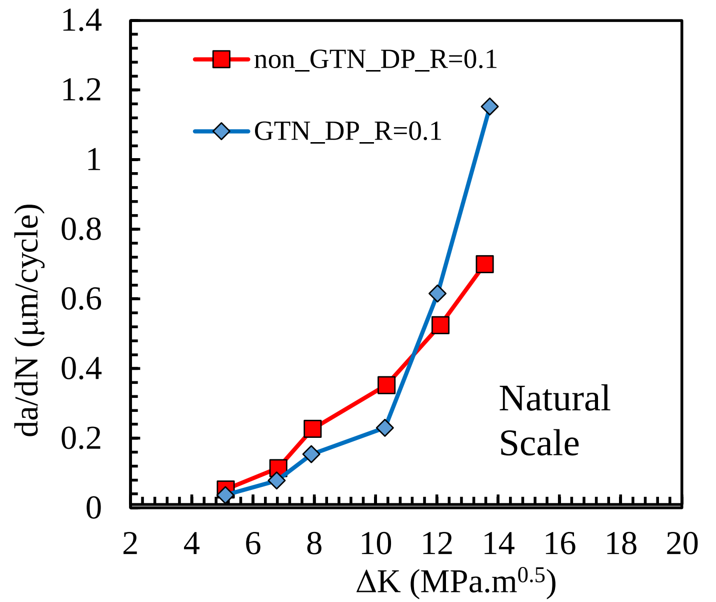

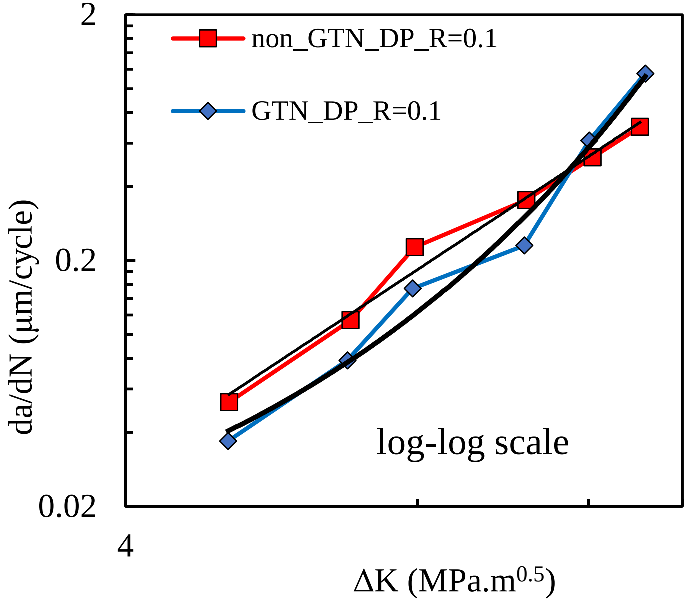

Plastic Strain at the crack tip

- To explain the influence of the GTN model on the FCGR, plastic strain was obtained, on the node located at the crack tip, for two distinct initial crack lengths (a_0).
- Higher initial crack lengths result in higher ΔK's at stable propagation zone.
- For a_0=11.5 mm, the numerical model considering GTN predicts a **slower** crack propagation rate.
- For a_0=21.5 mm, the numerical model considering GTN predicts a **faster** crack propagation rate, thus there is an inversion point between these two crack lengths.

Plastic Strain at the crack tip

- For both initial crack lengths, the plastic strain at the beginning of each propagation, is **higher** when GTN is considered.
- While for a_0=11.5 mm the plastic strain increases faster without GTN, this trend is reversed for a0=21.5 mm.
- The same trend is repeated for the remaining propagations of the crack growth.

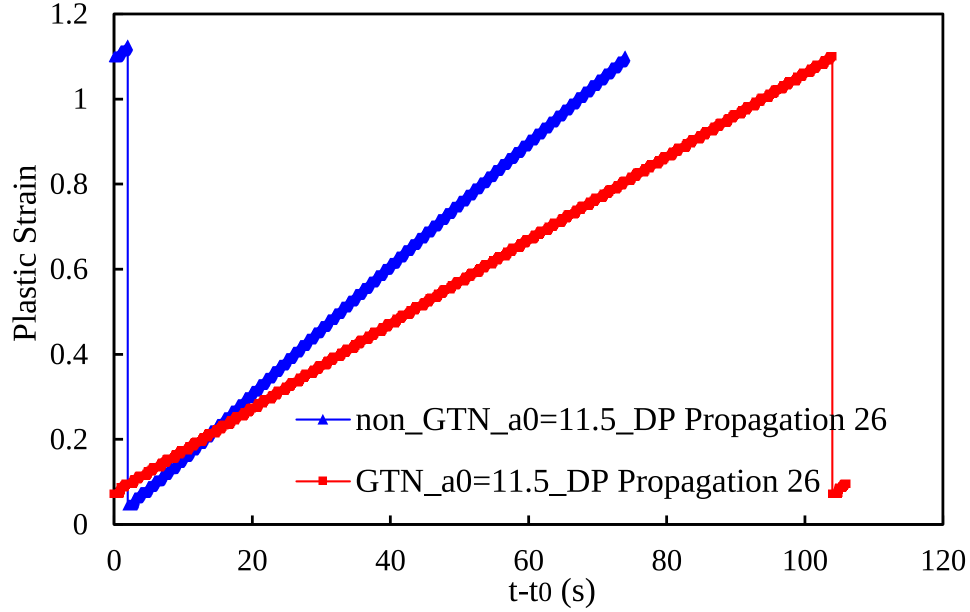

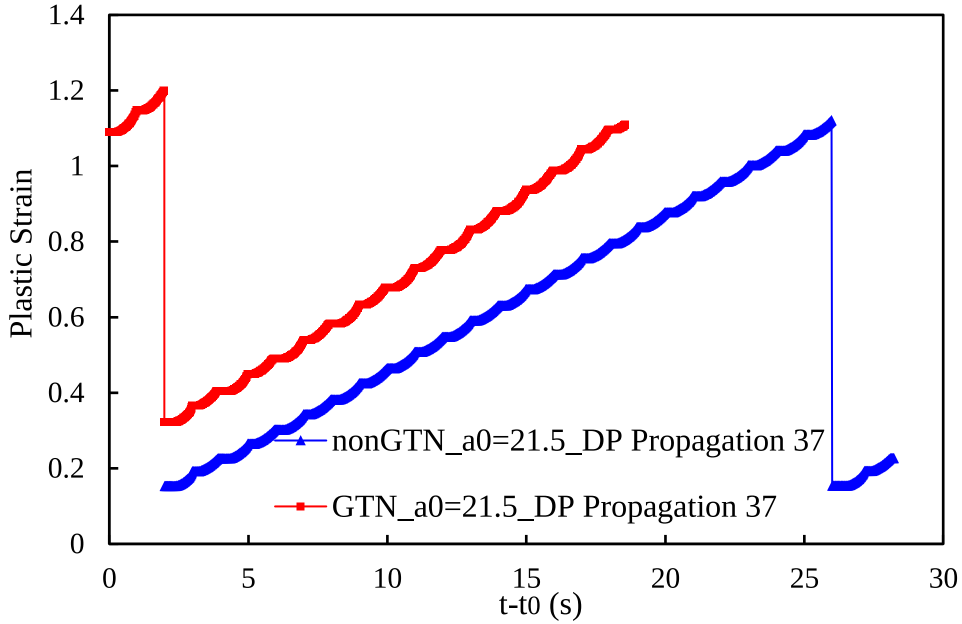

Plastic Strain at the crack tip

- The same analysis was performed in the last load cycle before the propagations referred in the previous slide.
- The same trend is followed. At the entrance of the last load cycle the model considering GTN provides a higher plastic strain.
- The increase in plastic strain is faster without GTN for a_0=11.5 mm, being this behavior reverted for a_0=21.5 mm.

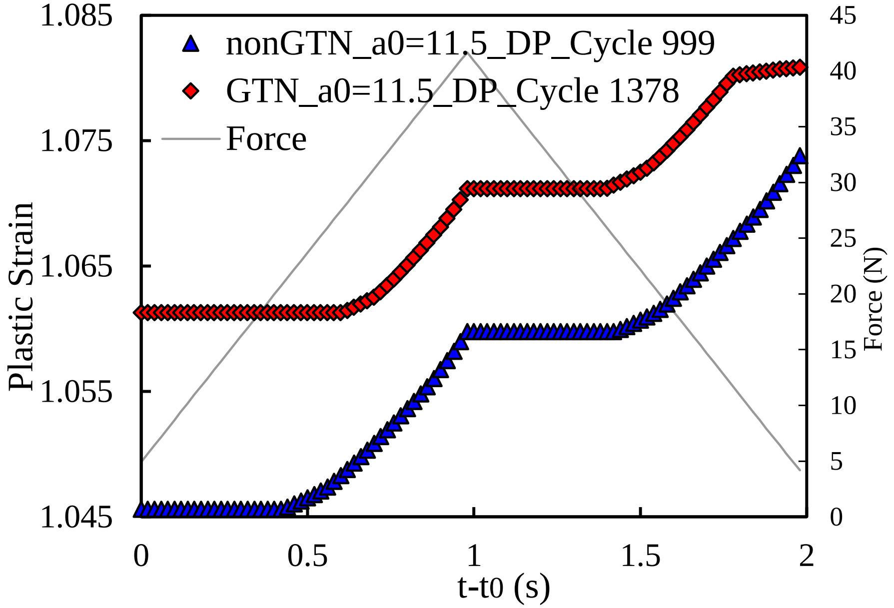

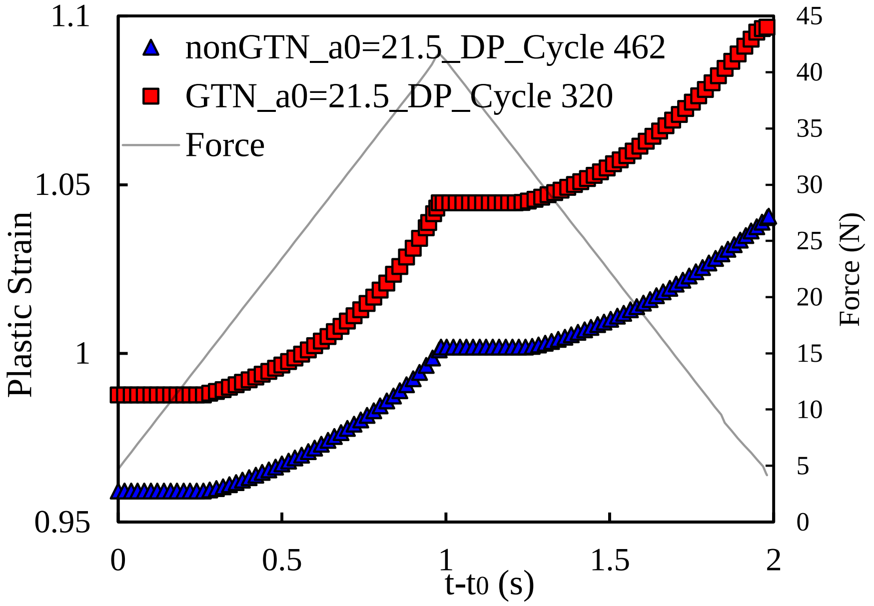

Crack Closure

- The CTOD analysis at the node behind the crack tip shows that the higher plastic strain induced by GTN results in higher closure levels.
- While for a_0=11.5 mm only the model with GTN shows closure at the last load cycle, for a_0=21.5 mm the crack closure ceases for both models.

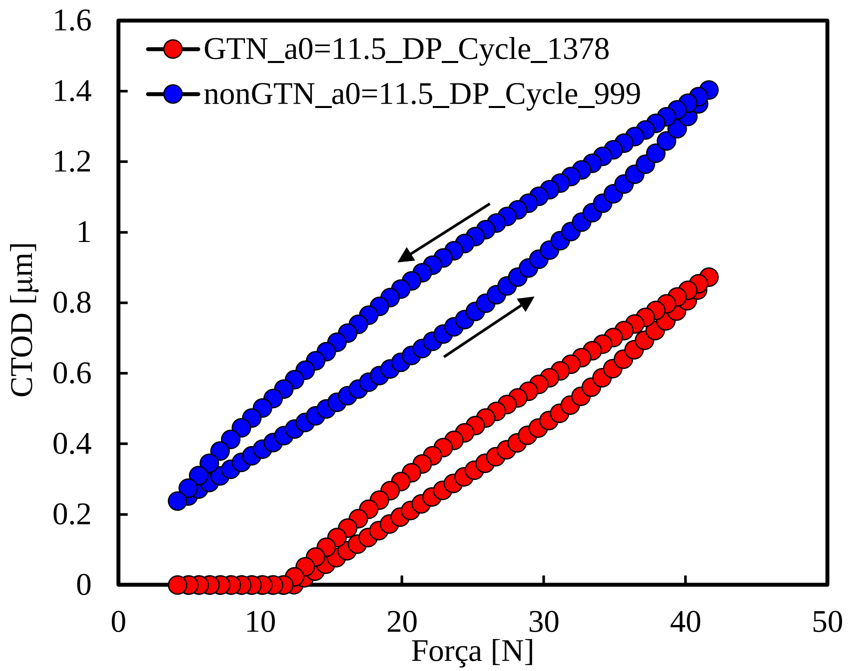

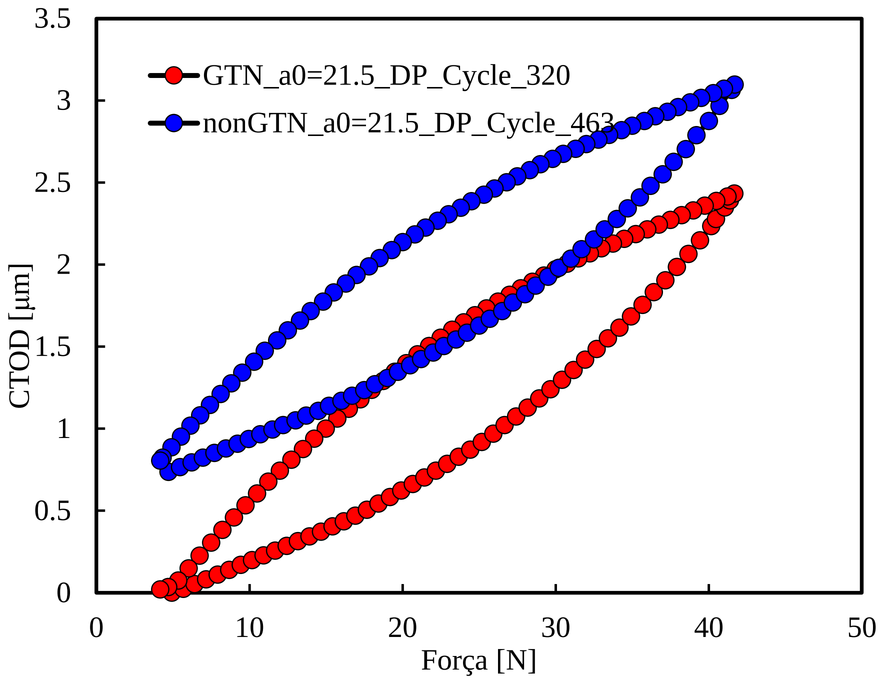

Crack Closure

- For a_0=11.5 mm crack closure is always larger with GTN, explaining the lower increase rate in plastic strain at the crack tip, and consequentially the lower FCGR.
- As for a_0=21.5 mm, at some point, the crack closure ceases to protect the material, the higher plastic strain achieved with GTN causes a faster FCGR.

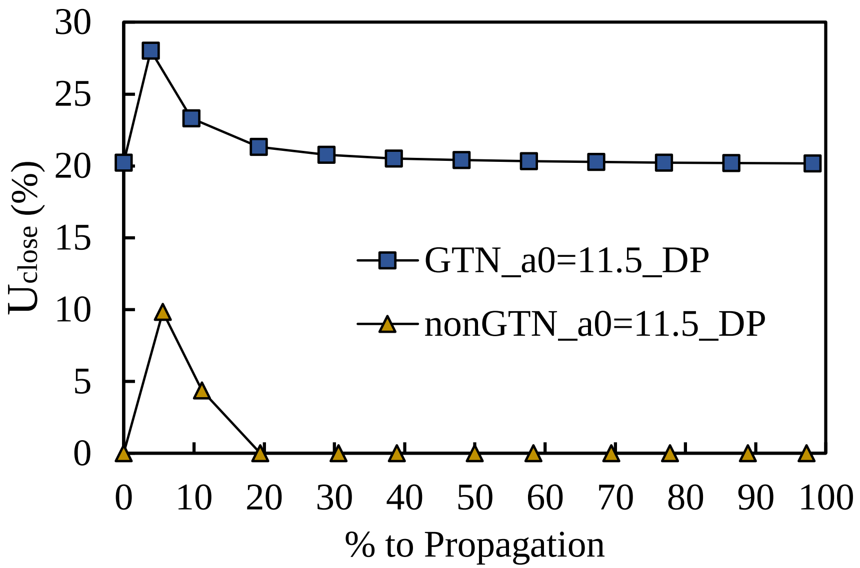

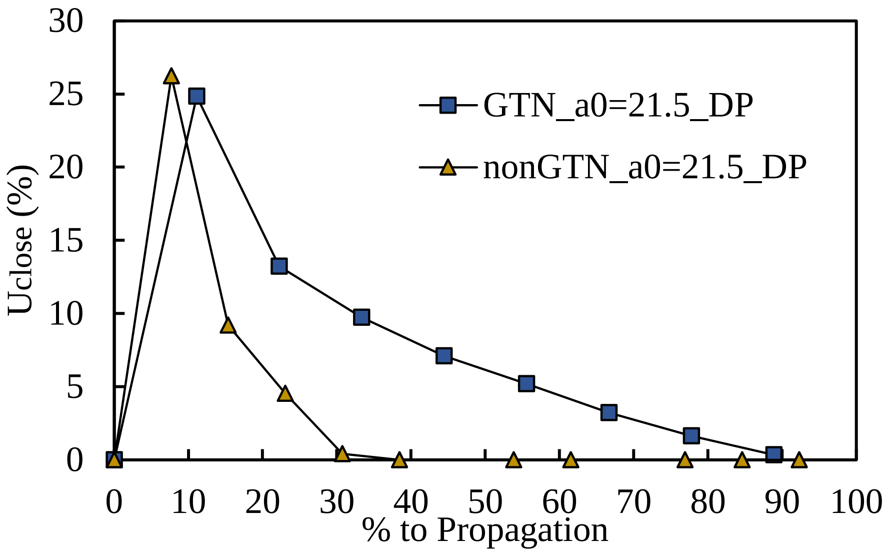

Crack Closure

- Crack closure was then disabled in the model considering GTN.
- For a_0=11.5 mm the plastic strain without crack closure is much higher. However, as the crack closure is alike for a_0=21.5 mm, with and without GTN, the da/dN-ΔK difference is small.

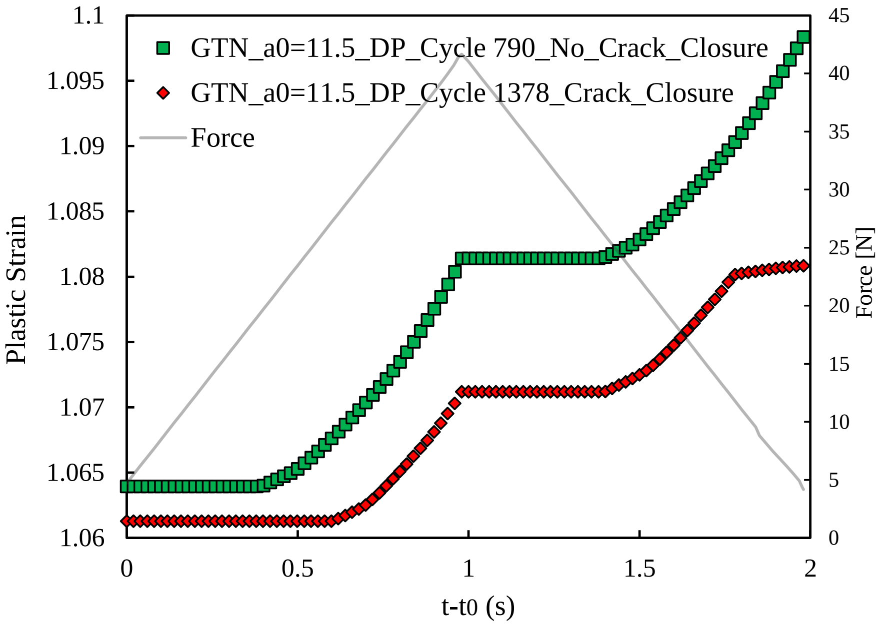

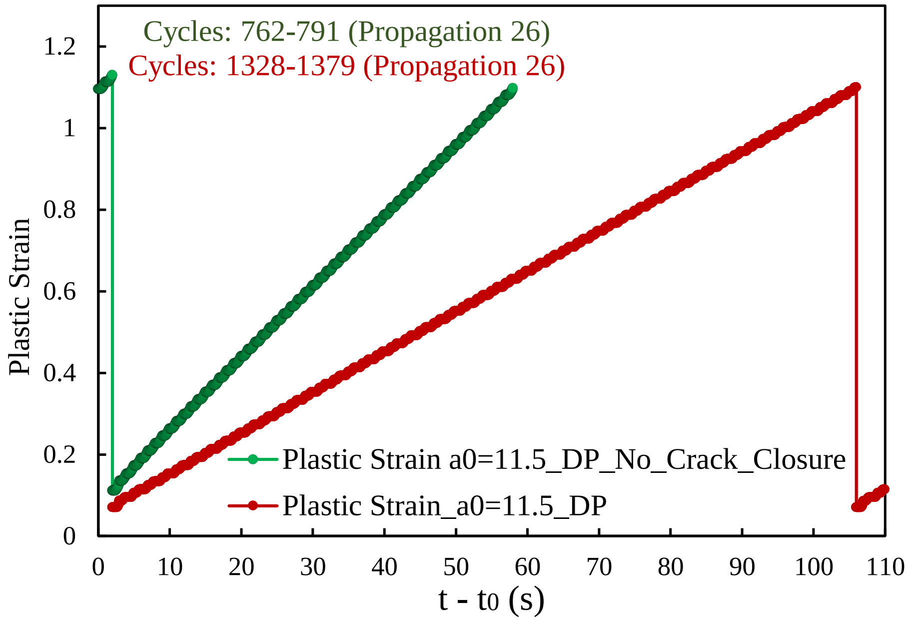

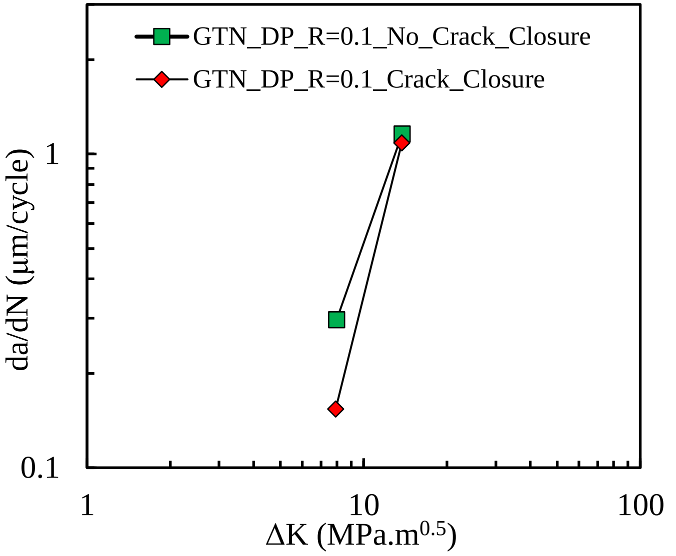

Conclusions

- Introducing the GTN in the already existent node release numerical model results in a tendency of the plastic strain to slide to higher levels.
- The higher plastic strain results in higher crack closure levels reverting the fragilization process and resulting in lower da/dN values.
- When crack closure ceases, at high ΔK's, the higher plastic strain levels results in the expected higher da/dN values.
- Crack closure is, this way, the fundamental crack tip mechanism leveling the da/dN behaviour of the models with and without GTN.

Acknowledgements

This research work was sponsored by national funds from the Portuguese Foundation for Science and Technology (FCT) under the project with reference PTDC/EME-EME/31657/2017 and by European Regional Development Fund (ERDF) through the Portugal 2020 program and the Centro 2020 Regional Operational Programme (CENTRO-01-0145-FEDER-031657) under the project MATIS (CENTRO-01-0145-FEDER-000014) and UIDB/00285/2020.

FCT Fundação para a Ciência e a Tecnologia   COMPETE 2020   PORTUGAL 2020   UNIÃO EUROPEIA Fundo Europeu de Desenvolvimento Regional

Thank you for your attention!